Deakin Research Online

Deakin University's institutional research repository

This is the authors final peer reviewed version of the item published as:

Dehghan-Manshadi, A., Barnett, Matthew and Hodgson, Peter 2007, Microstructural evolution during hot deformation of duplex stainless steel, *Materials science and technology*, vol. 23, no. 12, pp. 1478-1484.

Copyright : 2007, Institute of Materials, Minerals and Mining

Microstructural evolution during hot deformation of duplex stainless steel

A. Dehghan-Manshadi*, M. R. Barnett and P. D. Hodgson

The microstructure evolution during hot deformation of a 23Cr–5Ni–3Mo duplex stainless steel was investigated in torsion. The presence of a soft δ ferrite phase in the vicinity of austenite caused strain partitioning, with accommodation of more strain in the δ ferrite. Furthermore, owing to the limited number of austenite/austenite grain boundaries, the kinetics of dynamic recrystallisation (DRX) in austenite was very slow. The first DRX grains in the austenite phase formed at a strain beyond the peak and proceeded to <15% of the microstructure at the rupture strain of the sample. On the other hand, the microstructure evolution in δ ferrite started by formation of low angle grain boundaries at low strains and the density of these boundaries increased with increasing strain. There was clear evidence of continuous dynamic recrystallisation in this phase at strains beyond the peak. However, in the δ ferrite phase at high strains, most grains consisted of δ/δ and δ/γ boundaries.

Keywords: Duplex stainless steel, Hot deformation, EBSD, Dynamic recrystallisation

Introduction

Extensive studies of hot deformation and recrystallisation of steel have revealed the strong influence of the second phase on dynamic recrystallisation of austenite.[1,2] This influence is more obvious when the fraction of the second phase is large. One reason is that when the difference between the strengths of the austenite and the second phase (i.e. δ ferrite in this case) is significant, strain partitioning can play an important role in the dynamic recrystallisation (DRX) phenomenon. Decreasing the number of austenite/austenite grain boundaries, which are generally the most effective DRX nucleation sites, is also an important reason for this effect of the second phase. The role of these grain boundaries is more pronounced during the early stages of hot deformation, where the bulging of initial grain boundaries is the dominant recrystallisation mechanism.[3–7] Studies of DRX in duplex C–Mn and HSLA steels[8–10] have been complicated by the fact that deformation of the austenite encourages transformation to ferrite. Therefore, generally concurrent recrystallisation and transformation processes occur. Duplex (austenitic–ferritic) stainless steels with a matrix of austenite, a large fraction of δ ferrite and no phase transformation under certain deformation conditions appear to be suitable model alloys[11–16] for a more systematic investigation of the dynamic recrystallisation in the austenite/ferrite duplex microstructure.

Duplex stainless steels have been the subject of several hot deformation and annealing investigations.[16–21] The amount of each phase is related to the annealing temperature of the steel and can vary from 10 to 90%. The presence of a bcc ferrite phase, which has numerous slip systems and high stacking fault energy (SFE) in the vicinity of a fcc austenite phase with less slip systems and very low SFE, complicates the recrystallisation behaviour. For example, it has been shown[22] that the recrystallisation kinetics of austenite in the duplex structure is much lower than the recrystallisation kinetics in a single phase austenitic steel. Nonetheless, the dominant dynamic restoration mechanisms for ferrite and austenite are still dynamic recovery (DRV) and DRX respectively.[16,20,22,23]

The aim of the current work is to investigate the influence of the co-existence of a large volume fraction of δ ferrite on the dynamic restoration processes of austenite. In this respect, a duplex stainless steel with a similar volume fraction of δ ferrite and austenite has been selected for hot torsion tests. The dynamic restoration process of δ ferrite under those conditions was also studied in detail to assess whether they were affected by the hard second phase and the presence of ferrite–austenite boundaries.

Experimental methods

A duplex stainless steel with a composition of Fe–0·03C–2Mn–23Cr–5·5Ni–3Mo (wt-%) was used in the present study. Torsion samples with a gauge length of 20 mm and a diameter of 6·7 mm were machined from the initial 15 mm diameter bars. The torsion equipment used in the present study has been described elsewhere.[24] Soaking at 1200°C was used to achieve an initial homogenised microstructure. The soaking time of

---

Centre for Materials and Fibre Innovation, Deakin University, Waurn Ponds Vic. 3217, Australia

*Corresponding author, email adeh@deakin.edu.au

© 2007 Institute of Materials, Minerals and Mining
Published by Maney on behalf of the Institute
Received 6 February 2007; accepted 23 March 2007
DOI 10.1179/174328407X239019

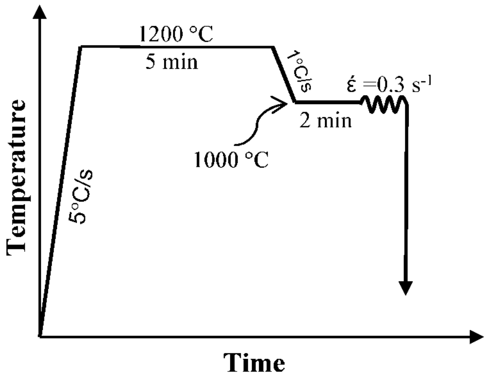

1 Schematic diagram of hot deformation tests

5 min at 1200°C appeared to establish a fully ferritic microstructure. The samples were then cooled at 1°C s^{-1} to 1000°C and held for 2 min, which resulted in a duplex structure with similar volume fractions of austenite and δ ferrite. The samples with the duplex structure were deformed at a strain rate of 0·3 s^{-1} to different strains. For comparison, two samples were also deformed at 1200 and 1100°C at a similar strain rate.

To investigate the deformed microstructure, the samples were quenched immediately (<0·5 s) after deformation (Fig. 1). Metallographic observations were performed on tangential sections at a depth of ~100 μm below the gauge surface. The microstructure of mechanically polished surfaces was investigated by electron backscattered diffraction (EBSD) under an accelerating voltage of 20 kV, a working distance of 25 mm from the gun and an aperture size of 60 μm. The EBSD maps were analysed using HKL Technology channel 5 software. The grain/subgrain misorientation distribution, twin boundary frequency and linear intercepts were extracted from the EBSD maps. The linear intercept was measured in the bar rolling direction (perpendicular to the torsion direction).

Results

The undeformed microstructure (i.e. after soaking and cooling to a deformation temperature of 1000°C) consisted of austenite and δ ferrite phases with some evidence of alignment along the bar rolling direction (Fig. 2). This volume fraction varied depending on the cooling temperature after the soaking. However, at 1000°C, ~50% of each phase was present in the microstructure. The austenite phase had a large fraction of high angle grain boundaries (>80%) with twin relationship, with no low angle grain boundaries (LAGB) observed (Fig. 3). In contrast, the δ ferrite phase contained a subgrain structure with an average δ/δ boundary misorientation of <15°. The frequency of high angle grain boundaries (HAGB) in this phase was very low (Fig. 3).

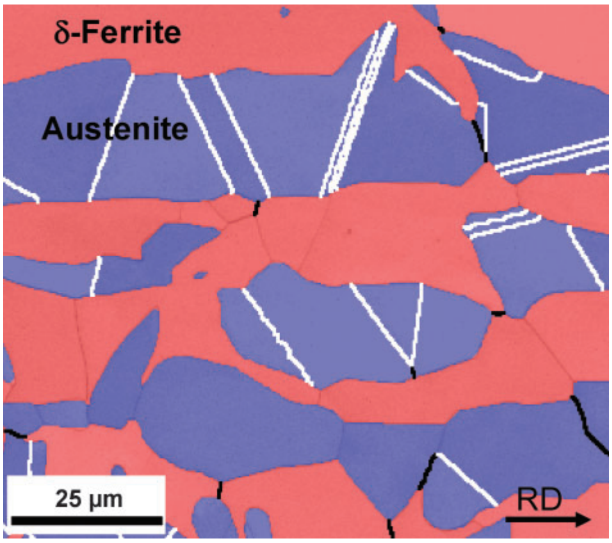

2 Electron backscattered diffraction phase map of undeformed sample after soaking at 1200°C and cooling to 1000°C: high angle (θ>15°) and twin boundaries shown by black and white lines respectively

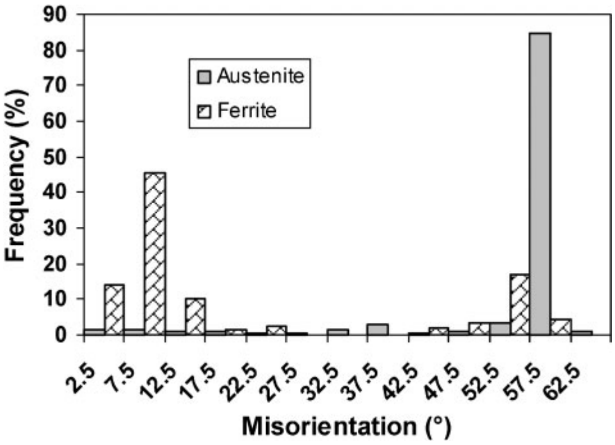

3 Misorientation distribution of undeformed microstructure for both phases of austenite and δ ferrite

The flow curve at T=1000°C and $\dot{\varepsilon}$=0·3 s^{-1} consisted of a strengthening stage (work hardening) to a peak stress, after which it started to decrease with further deformation (work softening). However, a steady state flow stress was never observed after the softening stage and the stress decreased continuously to the rupture of the sample (Fig. 4). The stress at rupture was very close to the initial yield and therefore, indicated significant softening in the material. The peak was much more evident at 1000°C than at the higher temperature, where there was a low level of work hardening and little work softening beyond the peak.

At very low strains, a particular shape of flow curve, i.e. a yield point-like phenomenon, was apparent. Increasing the deformation temperature extended this

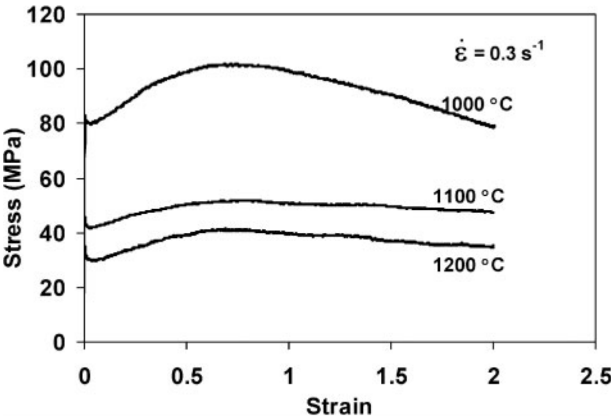

4 Flow curves of present steel at different deformation conditions and strain rate of 0·3 s^{-1}

particular area in the flow curve (Fig. 4). The presence of this specific shape of the early section of the flow curve, which in many ways resembles yield point phenomena in aged ferrite at room temperature with no (or limited) work hardening after the yield point, has been ascribed to the strain partitioning in the early stages of hot deformation.[19] The partitioning of alloying elements between these two phases, especially the interstitial nitrogen, and the effect of these elements on the restoration processes of each phase can further increase this difference in the two phases.[19] It has been suggested[19] that at the first stage of hot deformation, most of the strain is concentrated in the δ ferrite phase with no, or limited, load transfer across the interface from ferrite to austenite and therefore, the strengthening of the material is controlled by dynamic recovery (DRV) of this phase, leading to a constant flow stress. Increasing the strain can cause load transfer from the ferrite to austenite to maintain continuity. Owing to the higher strengths in the austenite, the result of this load transfer was appeared with increasing flow stress of the material. The presence of this flow curve behaviour has been reported by others[19,22] for wrought duplex stainless steels. However, the presence of this special shape of flow curve at 1200°C, where the microstructure is fully ferritic, suggests that this cannot be the sole responsible mechanism and hence, this is still an area that requires further investigation.

The microstructure of samples, deformed to different strains followed by rapid water quenching, was analysed by EBSD (Fig. 5). At a low strain ($\varepsilon=0{\cdot}25$), some substructure was formed in the δ ferrite phase with no obvious change observed in the austenite (Fig. 5*a*). Increasing the strain to 0·5 resulted in some grain elongation in both phases, with more low angle grain boundaries formed in the δ ferrite phase, while some twin boundaries in the austenite phase started to deviate from their initial twin crystallographic relationship (Fig. 5*b*). Furthermore, a low quantity of LAGBs formed within the austenite grains, although their quantity was very low compared to the ferrite phase. At a higher strain of 0·75 (Fig. 5*c*), which is close to the peak strain, a complete network of substructure along with some high angle grain boundaries was formed in the δ ferrite. At this strain, most of the twin boundaries in the austenite lost their twin relationship and changed to serrated high angle grain boundaries.

The elongation of both ferrite and austenite grains was increased as the strain was increased to 1·0. Also, the subgrain size in the δ ferrite increased while on the other hand, a large number of HAGBs were formed in this phase (Fig. 5*d*). At this strain, a large number of LAGBs were formed in the austenite phase, while a limited number of new DRX grains developed on the deformed twin or at the δ/γ interphase boundaries. The quantity of these new DRX grains increased with increasing strain (Fig. 5*e*). The final microstructure at a strain of 1·5 consisted of a δ ferrite phase with a very strong HAGB network and an austenite phase comprising some small DRX grains along with a very high quantity of LAGBs with a fine spacing between them. The volume fraction of recrystallised grains in the austenite was <15% at the rupture strain.

Discussion

The coexistence of a hard austenite phase and a soft δ ferrite phase during hot deformation led to a complicated deformation and restoration processes in this duplex structure. Under the hot deformation condition tested here (i.e. $T=1000^\circ\mathrm{C}$ and $\dot{\varepsilon}=0{\cdot}3\ \mathrm{s}^{-1}$), the flow curve shows a work hardening region and a peak stress followed by a softening stage. At the same time, the microstructure showed strong evidence for the evolution of DRV in both phases, with a limited amount of DRX in the austenite at strains of 1 and above. The volume fraction of DRX grains in austenite changed from 5% at a strain of 1·0 to ~15% at the fracture strain (Fig. 5), which is very low compared to the DRX fraction in a single phase austenitic stainless steel under similar deformation conditions.[5] At higher temperatures (for example, 1100°C in Fig. 4), the flow curve was similar to that for ferritic stainless steels[25,26] and also warm worked IF steel,[27] where a monotonic hardening to a steady state plateau (without a major peak) is observed. This is believed to be due to equilibrium between dislocation generation and annihilation (DRV), although at large strains, some flow softening can also occur owing to the texture effects. The more pronounced peak at 1000°C for the duplex structure would normally suggest extensive DRV of the austenite and further transformation from austenite to δ ferrite during deformation. However, both of these features are not supported by the microstructure observations. At this stage, the mechanism for this softening has not been identified. What is clear, though, is that a simple law of mixture approach to the flow curve is not adequate. At large strains, even though the δ ferrite showed low work hardening, the austenite would have definitely work hardened (as evidenced by the start of DRX). Therefore, in a law of mixture approach, this would greatly increase the average stress above the as received level. In austenite with full DRX, the steady state stress is much higher than σ_0.

The microstructure development during hot deformation is considerably affected by strain partitioning and the nature of grain and interphase boundaries (Fig. 5). This microstructure development can be schematically summarised as shown in Fig. 6. This figure implies a strong difference between the microstructures developed in the ferrite and austenite phases. Furthermore, there is a considerable difference between the microstructures developed in each phase compared with an austenitic[4,5,28] or a ferritic[29–31] stainless steel with single phase structure.

The undeformed microstructure (Fig. 6*a*) consisted of successive layers of δ ferrite and austenite of nearly equivalent volume fractions. This microstructure is the result of repeated phase transformation of $\gamma\rightarrow\delta$ and again $\delta\rightarrow\gamma$. The microstructure of the initial bars consisted of almost 40% ferrite and 60% austenite distributed in successive layers. The heating of this microstructure to 1200°C and holding for 5 min (i.e. soaking) caused a phase transformation of $\gamma\rightarrow\delta$ and a fully ferritic microstructure was observed by quenching of the sample at the end of the soaking process. As has been proposed elsewhere,[32,33] the chemical composition of δ ferrite and austenite (specifically in terms of alloying elements of Cr, Ni and Mo) is different. On the other

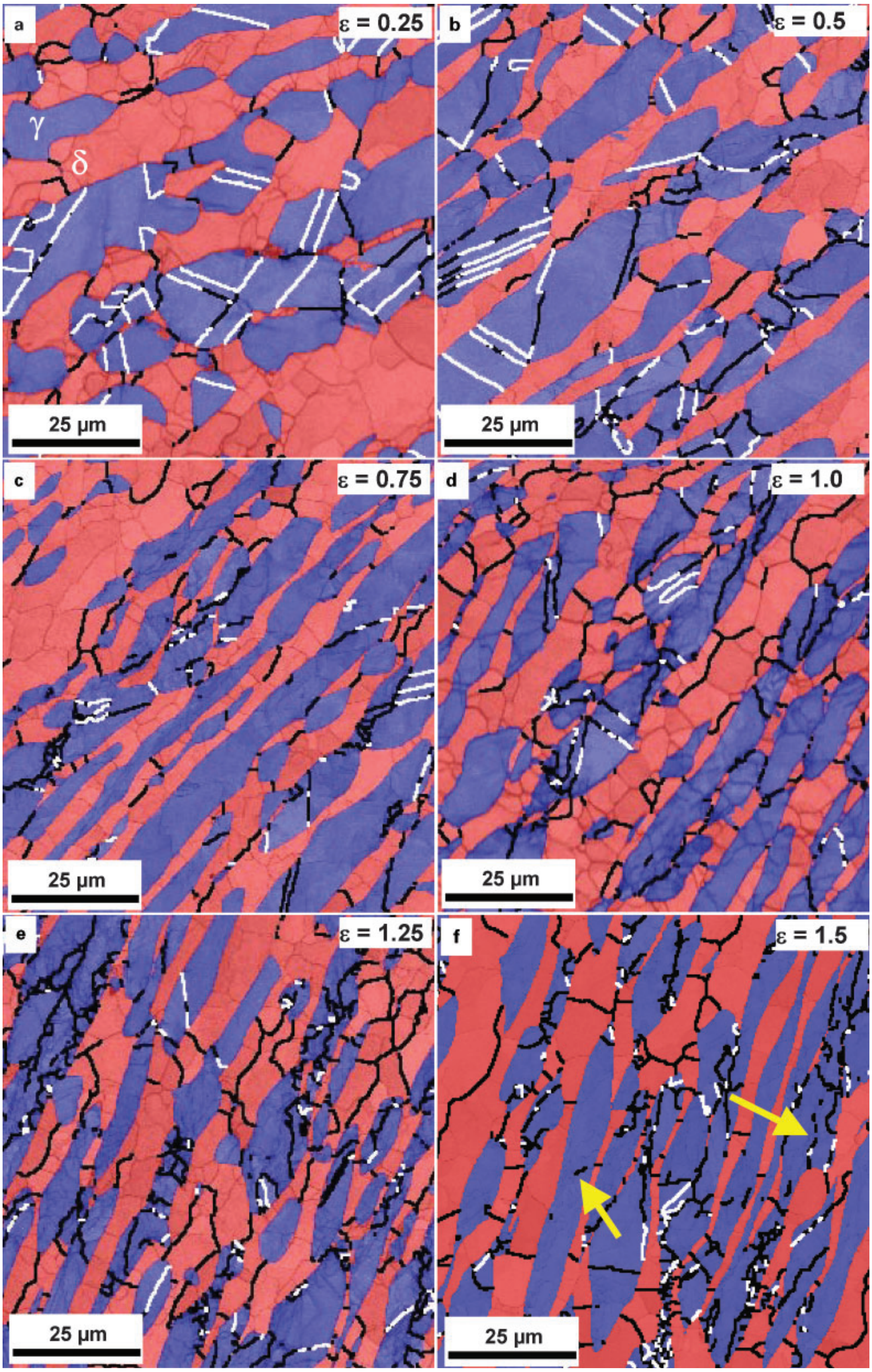

a ε=0·25; *b* ε=0. 5; *c* ε=0·75; *d* ε=1·0; *e* ε=1·25; *f* ε=1·5

5 Electron backscattered diffraction phase maps of samples after deformation at T=1000°C and $\dot{\varepsilon}$=0·3 s^{-1} to different strains followed by rapid water quenching: high angle (θ>15°) and twin boundaries shown by black and white lines respectively

hand, it seems that the soaking process used in the present study (i.e. 5 min at 1200°C) is not enough to change the distribution of alloying elements and homogenise the chemical composition. Therefore, the ferrite structure at the end of the soaking process would contain segregation of those elements in regions where the previous austenite phase existed. Those locations are then the preferred areas for transformation to austenite

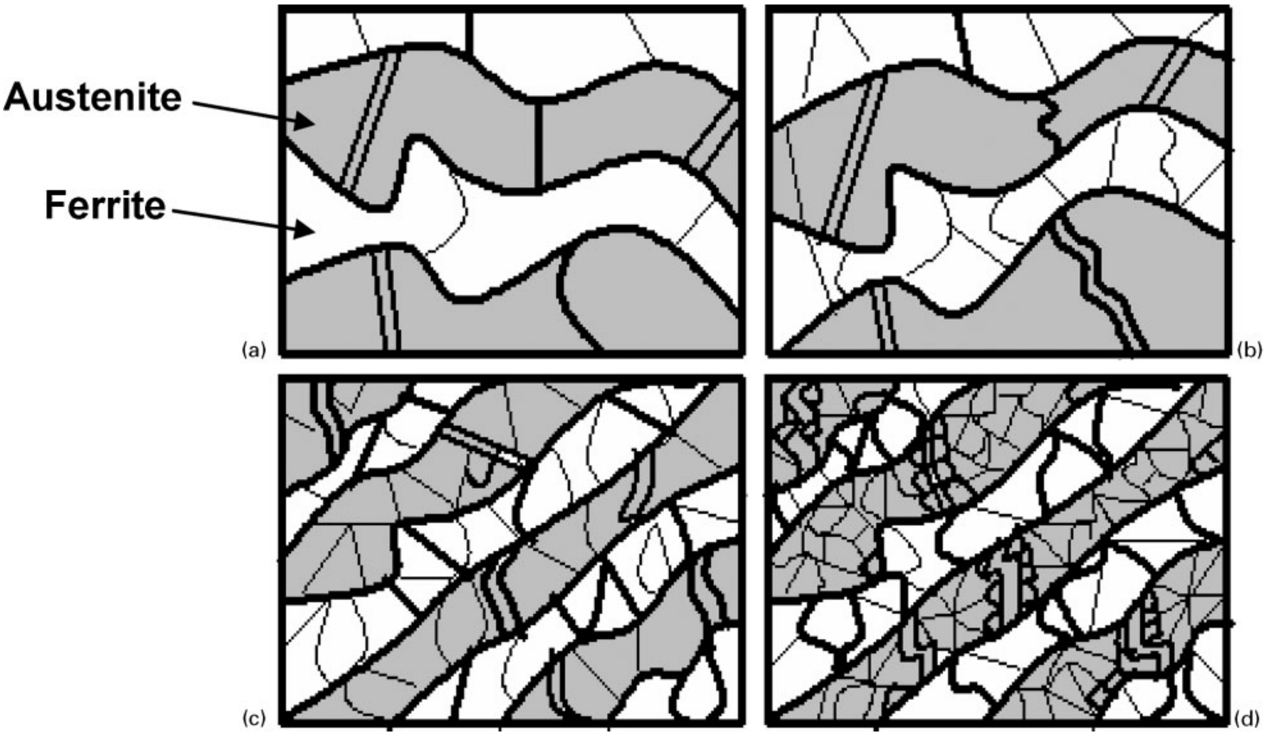

a $\varepsilon=0$; *b* $\varepsilon<\varepsilon_p$; *c* $\varepsilon=\varepsilon_p$; *d* $\varepsilon>\varepsilon_p$

6 Schematic illustration of microstructural development during hot deformation of duplex stainless steel: — LAGB, — HAGB

during cooling. Therefore, the microstructure after cooling again consisted of successive layers of ferrite and austenite.

The volume fraction of each phase remained constant during hot deformation under the present deformation condition, meaning that no phase transformation has occurred. Most of the γ boundaries have twin crystallography and no LAGBs are observed in this phase. However, the limited internal boundaries in the δ phase have a low misorientation. These LAGBs are likely to form owing to the recovery of dislocation formed from the internal stress during phase transformation or may have remained from the initial structure of the rolled bars. The δ/γ interphase grain boundaries have misorientations of about $40\pm5°$.

The microstructure evolution during hot deformation of this duplex structure started by the formation of LAGBs in the δ ferrite without any major influence on the austenite at strains lower than the peak (Fig. 6*b*). These LAGBs are the result of DRV as the dominant restoration mechanism in ferrite. By increasing deformation to the peak strain (Fig. 6*c*), more LAGBs are formed in the δ phase. These LAGBs evolve and lead to the gradual build-up of higher misorientation between the neighbouring subgrains (Fig. 7). The mean grain/subgrain size in the δ ferrite phase started to increase with further deformation after the peak strain (*see* Fig. 8), as a result of the evolution LAGBs to HAGBs. The increase in δ ferrite subgrain size appears to be proportional to the increase in the average misorientation of sub-boundaries (Fig. 7) in that phase.[34]

This phenomenon of changing from subgrains to grain boundaries is known as continuous dynamic recrystallisation[35,36] or extended recovery[23] and proceeds with increasing deformation (Fig. 6*d*). Although the exact mechanism of microstructural evolution during this continuous DRX (or extended recovery) is not fully understood, an increase in the misorientation of low angle grain boundaries[37–39] and coalescence and growth of subgrain boundaries[37,40,41] have been associated with this process. However, researchers have shown[21,34,42–44] that subgrain growth does not explain the rapid increase in the misorientation during continuous DRX (as observed in Fig. 7) and other mechanisms are likely to contribute to this phenomenon. However, the concurrent increase in the average misorientation of sub-boundaries (Fig. 7) with an increase in the average subgrain size (Fig. 8) followed by the formation of high angle grain boundaries (DRX) is obvious in the current work (δ ferrite phase). This is consistent with the evolution of DRX in ferrite (i.e.

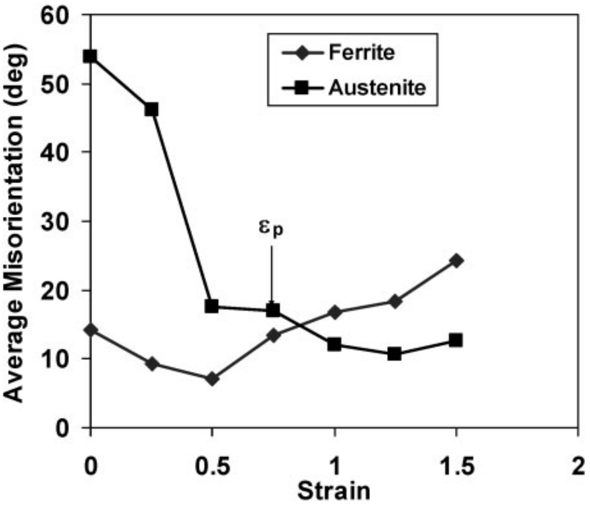

7 Average misorientation (θ>2°) of each boundary as function of strain

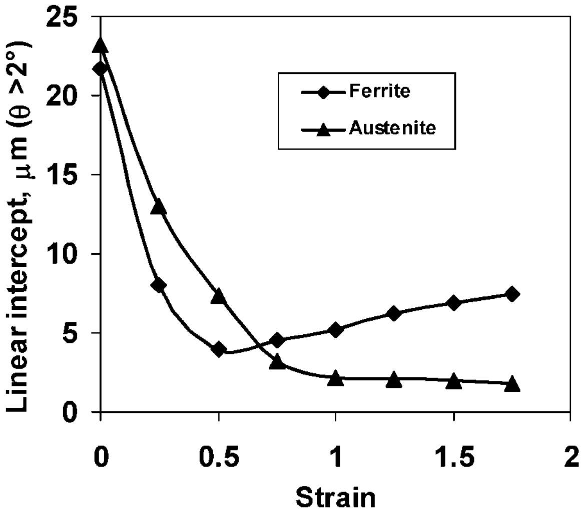

8 **Change in linear intercept of boundaries in γ and δ phases (*θ* >2°)**

continuous DRX) based on the proposed mechanisms. The result of this DRX phenomenon is the replacement of the LAGB network by a HAGB structure with an average misorientation of ~30° and in comparison to the austenite, a relatively large cell size.

An important observation, though, is that there are very few actual grains in the *δ*ferrite phase and most of the grains have both *δ*/*δ* and *γ*/*δ* boundaries. In this case, there is an added complexity. Increasing the deformation decreases the thickness of the *δ* ferrite layers. Because these are of a similar thickness to the size of the subgrain, it means that the *δ*/*γ* boundaries will also be sinks for dislocation as well as the traditional *δ*/*δ* subboundaries. This also means that dislocations will have different boundaries for their generation. The fact that the width is decreasing with increasing strain which the average subgrain size is increasing means that the ratio of *δ*/*δ* and *δ*/*γ* boundaries will change with strain.

The microstructural change and restoration process in the austenite phase is different from the above observations in *δ* ferrite. Because strain accommodation in austenite is less than that in *δ* ferrite (at least at the early stages of deformation), limited LAGBs are observed in this phase at low strains (Fig. 6*b*). The first evidence of DRX (the dominant restoration mechanism of austenite) is observed at a strain higher than the peak in the flow curve by nucleation of DRX grains on the deformed twin or *δ*/*γ* interphase boundaries. The formation of new DRX grains and LAGBs increased with increasing strain and in contrast to ferrite, where the grain/subgrain network size started to increase with increasing strain from the peak, the grain/subgrain size decreased continuously with increasing strain (Fig. 7).

In contrast to ferrite, some discrete austenite grains (i.e. grains with only *γ*/*γ* boundaries) were observed in this phase (e.g. Fig. 5*e*). These actual grains were mostly formed on the serrated initial grain (twin) boundaries, indicating discontinuous DRX. However, as for ferrite, some regions of austenite showed an increase in the misorientation of segments of LAGBs. Those segments then changed to HAGBs, indicating a continuous type of recrystallisation in austenite. The arrows in Fig. 5*f* show examples of such segments.

An important difference between DRX in the austenite phase of a duplex structure and a single phase austenitic stainless steel is in the role of grain boundary serration and the bulging of new DRX grains on these serrated boundaries. While grain boundary serration and bulging is the most important DRX mechanism in the single phase austenitic steels[3,5] (at least for the early stages of recrystallisation), this phenomenon is not often observed in the duplex structure, owing to the limited number of austenite/austenite grain boundaries. However, where these boundaries did exist they were the sites for new DRX grains on the serrated *γ*/*γ* boundaries.

The volume fraction of DRX grains increased with increasing deformation although it was still very low at the strain of fracture. This means that more strain is needed to complete the DRX process in the austenite phase for this structure. However, this limited fraction of DRX in the austenite phase cannot be the sole reason for the appearance of the peak in the flow curve. The softening of *δ* ferrite phase, due to DRV and continuous DRX, can be considered as another possible mechanism causing the peak to appear in the flow curve. It seems that the rotation of microstructure from layers/stringers parallel to the torsion axis (Fig. 2) to an almost 60° with the torsion axis (Fig. 5) can accelerate the ferrite softening, owing to strain partitioning between the ferrite and the austenite.

Conclusions

Hot deformation of a duplex stainless steel, with equal volume fractions of *δ* ferrite and austenite in the initial microstructure, was examined in torsion. The flow curve showed a work hardening stage and a peak strain followed by gradual increase to the rupture of the sample. A very particular shape of flow curve, i.e. a yield point, was observed at the early stages of deformation, although the mechanism for this was not clear.

The microstructure evolution during hot deformation was very different in each phase. While the evidence of continuous DRX, i.e. gradual increase in misorientation and distance of low angle grain boundaries, was observed in *δ* ferrite, the formation of new DRX grains on deformed twin boundaries or *γ*/*δ* interphase boundaries appeared in austenite phase (conventional DRX). However, owing to limitation in the number of austenite/austenite boundaries, the evolution of DRX in austenite was limited.

References

1. F. J. Humphreys and M. Hatherly: 'Recrystallization and related annealing phenomena', 1st edn, 497; 1996, Oxford, Pergamon.
2. E. Hornbogen and U. Koster: in 'Recrystallization of metallic materials', (ed. F. Haessner), 159–194; 1978, Stuttgart, Riederer.
3. E. Brunger, X. Wang and G. Gottstein: *Scr. Mater.*, 1998, **38**, 1843–1849.
4. A. Belyakov, H. Miura and T. Sakai: *Mater. Sci. Eng. A*, 1998, **A255**, 139–147.
5. A. Dehghan-Manshadi, H. Beladi, M. R. Barnett and P. D. Hodgson: *Mater. Forum*, 2004, **467–470**, 1163–1168.
6. G. Gottstein, E. Brunger and D. Ponge: Proc. Conf. on 'Advanced in hot deformation textures and microstructures', Pittsburgh, PA, USA, October 1993, TMS, 477–492.
7. T. Sakai: *J. Mater. Process. Technol.*, 1995, **53**, 349–361.
8. C. M. Sellars: Proc. Conf. on 'Hot working and forming processes', London, UK, July 1979, The Metals Society, 3–15.
9. C. M. Sellars: *Czech. J. Phys. B*, 1985, **35B**, 239–248.
10. P. D. Hodgson, D. C. Collinson and B. A. Parker: Proc. Conf. on 'Advances in hot deformation textures and microstructures', USA, 41–61; 1994, Pittsburgh, PA, TMS.

11. K. Tsuzaki, H. Matsuyama, M. Nagao and T. Maki: *Mater. Trans. JIM*, 1990, **31**, 983–994.
12. M. Blicharski: *Met. Sci.*, 1984, **18**, 99–102.
13. N. Akdut and J. Foct: *ISIJ Int.*, 1996, **36**, 883–892.
14. J. M. Cabrera, A. Mateo, L. Llanes, J. M. Prado and M. Anglada: *Mater. Sci. Technol.*, 2003, **143–144**, 321–325.
15. H. J. McQueen, E. Evangelista and N. D. Ryan: Proc. Conf. on 'Thermomechanical processing: mechanisms, microstructure and control', Sheffield, UK, June 2002, University of Sheffield, 359–367.
16. O. Balancin, W. A. M. Hoffmann and J. J. Jonas: *Metall. Mater. Trans. A*, 2000, **31A**, 1353–1364.
17. J. A. Jimenez, M. Carsi and O. A. Ruano: *J. Mater. Sci.*, 2000, **35**, 907–915.
18. W. Reick, M. Pohl and A. F. Padilha: *ISIJ Int.*, 1998, **38**, 567–571.
19. L. Duprez, B. C. De Cooman and N. Akdut: *Metall. Mater. Trans. A*, 2002, **33A**, 1931–1938.
20. T. Maki, T. Furuhara and K. Tsuzaki: *ISIJ Int.*, 2001, **41**, 571–579.
21. K. Tsuzaki, X. Huang and T. Maki: *Acta Mater.*, 1996, **44**, 4491–4499.
22. A. Iza-Mendia, A. Pinol-Juez, J. J. Urcola and I. Gutierrez: *Metall. Mater. Trans. A*, 1998, **29A**, 2975–2986.
23. P. Cizek and B. P. Wynne: *Mater. Sci. Eng. A*, 1997, **A230**, 88–94.
24. H. Weiss, D. H. Skinner and J. R. Everett: *J. Phys. E*, 1973, **6E**, 709–712.
25. E. V. Konopleva, M. Sauerborn, H. J. McQueen, N. D. Ryan and R. G. Zaripova: *Mater. Sci. Eng. A*, 1997, **A234–236**, 826–829.
26. E. Nes: *Acta Metall. Mater.*, 1995, **43**, 2189–2207.
27. A. Oudin, M. R. Barnett and P. D. Hodgson: *Mater. Sci. Eng. A*, 2004, **A367**, 282–294.
28. N. D. Ryan, H. J. McQueen and E. Evangelista: Proc. 7th Int. Symp. on 'Metallurgy and materials science', Roskilde, Denmark, September 1986, Riso National Laboratory, 527–534.
29. A. Belyakov, O. Kaibyshev and T. Sakai: *Metall. Mater. Trans. A*, 1998, **29A**, 161–167.
30. F. Gao, Y. Xu and K. Xia: *Metall. Mater. Trans. A*, 2000, **31A**, 21–27.
31. H. Yagi, N. Tsuji and Y. Satio: *Tetsu-to-Hagane*, 2000, **86**, 65–72.
32. T. H. Chen and J. R. Yang: *Mater. Sci. Eng. A*, 2001, **A311**, 28–41.
33. S. Herenu, I. Alvarez-Armas and A. F. Armas: *Scr. Mater.*, 2001, **45**, 739–745.
34. X. Huang, K. Tsuzaki and T. Maki: *Acta Metall. Mater.*, 1995, **43**, 3375–3384.
35. T. Sakai, A. Belyakov and H. Miura: Proc. 1st Joint Int. Conf. on 'Recrystallization and grain growth', Aachen, Germany, 2001, Springer-Verlag, 669–682.
36. S. Gourdet, C. Chovet and F. Montheillet: Proc. 4th Conf. on 'Recrystallization and related phenomena', Tsukuba Japan, July 1999, The Japan Institute of Metals, 259–264.
37. R. K. Davies, V. Randle and G. J. Marshall: *Acta Mater.*, 1998, **46**, 6021–6032.
38. H. Jazaeri and F. J. Humphreys: *Mater. Sci. Forum*, 2002, **396–402**, 551–556.
39. O. Engler and M. Y. Huh: *Mater. Sci. Eng. A*, 1999, **A271**, 371–381.
40. R. H. Bricknell and J. W. Edington: *Acta Metall.*, 1979, **27**, 1303–1311.
41. E. Nes: *J. Mater. Sci. Lett.*, 1978, **13**, 2052.
42. S. J. Hales and T. R. McNelley: *Acta Metall.*, 1988, **36**, 1229–1239.
43. K. Tsuzaki, H. Matsuyama, M. Nagao and T. Maki: *Mater. Trans. JIM*, 1990, **31**, 983–994.
44. H. Gudmundsson, D. Brook and J. A. Wert: *Acta Metall. Mater.*, 1991, **29**, 19–35.